tion $c > c_2$. Above $c_2 = 0.07\%$ the fast mode is approximately constant while the slow mode is approximately proportional to $1/c$, as predicted by Doi and Edwards. Table I also shows calculated values of D_r for the rod structure 15000 × 20 Å. The calculated values are several orders of magnitude smaller than experiment. However, the Doi-Edwards theory does not take account of electrostatic repulsions, and this could account partially for the discrepancies.

Based on the above discussion, it is not possible to make a clear choice as to the origin of the hydrodynamic transition observed in xanthan solutions at $c \sim c_2$. It seems likely that the charged xanthan molecule has a semirigid structure, and therefore a quantitative application of the Doi-Edwards theory is not justified. It is pertinent to note, however, that Lee et al.[26] have argued that the hydrodynamics of congested solutions of semiflexible chains can be treated by a dynamical equation equivalent to that of Doi and Edwards, again leading to the prediction of bimodal decays in the dynamic structure factor. On the other hand, a broken-rod structure of xanthan would lead to intermolecular contacts along localized sequences and thus facilitate the formation of junction zones.

Note Added in Proof. Subsequent experiments, in which the diffusion of latex microspheres in semidilute xanthan solutions was studied, are consistent with the existence of a motionally restricted isotropic network of long thin fibers. This suggests that the Doi-Edwards theory should be applicable in the range $1.0 < c < 3.5$ g/L (Jamieson, A. M.; Southwick, J. G.; Blackwell, J. *J. Polym. Sci., Polym. Phys. Ed.*, submitted). The quantitative discrepancy between theory and experiment noted above implies that the critical entanglement length for onset of constrained diffusion is substantially smaller than the whole rod length. This effect has been observed for other rodlike macromolecules (Jain, S.; Cohen, C. *Macromolecules* **1981**, *14*, 759).

Acknowledgment. This research was supported by NSF Grant No. PCM-18631.

References and Notes

(1) Jansson, P. E.; Keene, L.; Lindberg, B. *Carbohydr. Res.* **1975**, *45*, 275.
(2) Melton, L. D.; Mindt, L.; Rees, D. A.; Sanderson, G. R. *Carbohydr. Res.* **1976**, *46*, 245.
(3) Sandford, P. A.; Watson, P. R.; Knutson, C. A. *Carbohydr. Res.* **1978**, *63*, 253.
(4) Cadmus, M. C.; Rogovin, S. P.; Burton, K. A.; Pittsley, J. E.; Knutson, C. A.; Jeannes, A. *Can. J. Microbiol.* **1976**, *22*, 942.
(5) Cadmus, M. C.; Knutson, C. A.; Lagoda, A. A.; Pittsley, J. E.; Burton, K. A. *Biotechnol. Bioeng.* **1978**, *20*, 1003.
(6) Whitcomb, P. J.; Macosko, C. W. *J. Rheol.* **1978**, *22*, 493.
(7) Rinaudo, M.; Milas, M.; Duplessix, R. *IUPAC 26th Symp. Macromol., Makro Mainz* **1979**, 800.
(8) Daoud, M.; Cotton, J. P.; Farnoux, B.; Jannink, G.; Sarma, G.; Benoit, H.; Duplessix, R.; Picot, C.; de Gennes, P. G. *Macromolecules* **1975**, *8*, 804.
(9) de Gennes, P. G. *Macromolecules* **1976**, *9*, 587.
(10) de Gennes, P. G. *Macromolecules* **1976**, *9*, 594.
(11) Schaefer, D. W.; Joanny, J. F.; Pincus, P. *Macromolecules* **1980**, *13*, 1280.
(12) Southwick, J. G.; McDonnell, M. E.; Jamieson, A. M.; Blackwell, J. *Macromolecules* **1979**, *12*, 305.
(13) Doi, M.; Edwards, S. F. *J. Chem. Soc., Faraday Trans. 2* **1978**, *74*, 560.
(14) Doi, M.; Edwards, S. F. *J. Chem. Soc., Faraday Trans. 2* **1978**, *74*, 918.
(15) Doi, M. *J. Phys. (Paris)* **1975**, *36*, 607.
(16) Holzwarth, G. *Biochemistry* **1976**, *15*, 4333.
(17) Southwick, J. G.; Jamieson, A. M.; Blackwell, J., submitted to *Carbohydr. Res.*
(18) Brown, J. C.; Pusey, P. N.; Dietz, R. *J. Chem. Phys.* **1975**, *62*, 1136.
(19) Pusey, P. N.; Koppel, D. E.; Schaefer, D. W.; Camerini-Otero, R. D.; Koenig, S. H. *Biochemistry* **1974**, *13*, 952.
(20) Flory, P. J. *Proc. R. Soc. London, Ser. A* **1956**, *234*, 73.
(21) Bawden, F. C.; Pirie, N. W. *Proc. R. Soc. London, Ser. B* **1937**, *123*, 274.
(22) Bernal, J. D.; Fankucken, I. *J. Gen. Physiol.* **1941**, *25*, 111.
(23) Oster, G. *J. Gen. Physiol.* **1950**, *33*, 445.
(24) Mitchell, J. R. In "Polysaccharides in Foods"; Blanshard, J. M. V., Mitchell, J. R., Eds.; Butterworth: London, 1979.
(25) Valenti, B.; Ciferri, A. *J. Polym. Sci., Polym. Lett. Ed.* **1978**, *16*, 657.
(26) Lee, W. I.; Schmitz, K.; Lin, S. C.; Schurr, J. M. *Biopolymers* **1977**, *16*, 583.

Reptation in Entangled Polymer Solutions by Forced Rayleigh Light Scattering

L. Léger,* H. Hervet, and F. Rondelez

Laboratoire de Physique de la Matière Condensée, Collège de France, 75231 Paris Cedex 05, France. *Received March 5, 1981*

ABSTRACT: We have measured the self-diffusion coefficient of polystyrene chains in benzene solutions as a function of both concentration C and molecular weight M, using a forced Rayleigh light scattering technique. In the semidilute regime where the chains overlap, we obtain $D_{self} \sim C^{-\alpha}M^{-\beta}$, with $\alpha = 1.7 \pm 0.1$ and $\beta = 2 \pm 0.1$, in good agreement with scaling and reptation predictions. Measurements on mixed systems, with labeled chains shorter than their neighbors, demonstrate for the first time the weakness of the tube renewal processes in semidilute polymer solutions.

Introduction

Entangled polymer solutions have very unusual viscoelastic behavior. Much effort, both experimental and theoretical, has been devoted to unravel their dynamical properties; however, they are not yet completely elucidated. The difficulty is to correctly take into account the effect of chain disentanglements. The recent scaling approach[1,2] has made a significant contribution to the understanding of chain dynamics by pointing out that a large class of motions, the so-called collective motions, do not require chain disentanglements.[3] Then, when performing a dynamic experiment, one has to distinguish carefully between collective and individual chain motions, i.e., monomer motions respectively without or with relative displacements of the center of mass of the chains. Both contributions are usually important, but some experiments allow separation of them. Following ref 3, the collective motions of the chains can be described in terms of a cooperative diffusive mode, characterized by a diffusion coefficient $D_{coop} \sim \xi^{-1}$, where ξ represents the average distance between entanglements. ξ is independent of the polymerization index N, and its concentration dependence can

0024-9297/81/2214-1732$01.25/0

easily be deduced from scaling arguments.[2,3] This description is in qualitative agreement with recent dynamic light scattering and sedimentation experiments. Small discrepancies remain between observed and predicted exponents for $\xi(C)$[4-7] but it has been argued that those differences could be attributed to the fact that the good-solvent limit is difficult to reach in the case of a dynamic quantity.[7,8] This hypothesis seems to be supported by recent sedimentation experiments in Θ-solvent conditions, which allow those convergence problems to be bypassed, and are in very good agreement with scaling predictions.[9]

The situation is far less clear for experiments where individual chain motions are important. For example, to describe the Brownian diffusion of the center of mass of the chains, one has to introduce a model taking into account the chain disentanglements. This is the aim of the reptation model,[10] which defines around each chain an effective tube made of all the topological constraints imposed on one chain by its neighbors. Since the chains cannot cross each other, each chain can easily slide along its tube while its motion in any other direction becomes very difficult. Following the scaling approach,[3] the average diameter of the tube is ξ. The reptation time T_R, i.e., the time for the chain to completely renew its configuration, can easily be evaluated, and $T_R \sim N^3C^{1.5}$ in the good-solvent limit. This prediction can be collated with experiments in several ways: (i) T_R represents the limit between the liquid-like ($t > T_R$) and the rubber-like ($t < T_R$) behavior; i.e., it is the longest relaxation time measured in a mechanical experiment. (ii) The zero-shear viscosity η_0 is related to T_R through $\eta_0 = G_0T_R$, where G_0 is the shear elastic modulus of the solution, independent of the molecular weight and proportional to the number of entanglements: $G_0 \sim 1/\xi^3$. A large amount of data is available,[23] with exponents for both molecular weight and concentration dependences usually larger than predicted. This discrepancy is, up to now, unexplained.

To try and elucidate that point, we have undertaken measurements of the self-diffusion coefficient of the chains, D_{self}, as a function of both molecular weight and polymer concentration. D_{self} presents many advantages over other dynamical quantities as it can be measured very close to equilibrium. On the other hand, self-diffusion experiments are not easy to perform in polymer solutions: D_{self} typically lies in the range 10^{-8}–10^{-9} cm^2/s and conventional tracer techniques are hardly workable (the diffusion over 1 cm is achieved in several months!). We have therefore developed a new technique, the forced Rayleigh light scattering (FRS) technique, which allows us to reduce the diffusion length down to a few microns and is quite well adapted to the study of polymer entanglements. Preliminary results have already been reported[11] demonstrating the feasibility of the experiment and establishing that the observed concentration dependence of D_{self} is compatible with scaling plus reptation predictions. In the present paper, we report on a more complete set of data on both concentration and molecular weight dependences of D_{self}. We describe the FRS techique in part I, present our results in part II, and compare with scaling and reptation predictions and other experimental results in part III.

I. Experimental Technique

The forced Rayleigh light scattering experiment (FRS) that we have developed to follow mass diffusion is a tracer technique in which the diffusion length can be reduced down to a few microns without any loss of accuracy. The principle of the experiment is the following: a few chains in the solution are labeled with a photochromic probe. A periodic distribution of photoexcited molecules is created by illuminating the sample with a pulsed interference pattern and is relaxed by diffusion after the flash excitation. This periodic distribution of photoexcited molecules acts as an absorption grating for a second laser beam only sensitive to the photoexcited species. The decrease of the diffracted intensity directly reflects the kinetics of the diffusion of the molecules.[12]

Table I
Characteristics of the Different Polystyrene Samples Used

M_w	M_w/M_n	C^*,[a] g/g
78 300	1.06	4×10^{-2}
271 000	1.10	1.5×10^{-2}
598 600	1.10	7.5×10^{-3}
754 000	1.12	

[a] Evaluated from $D_{self}(C)$ (Figure 5).

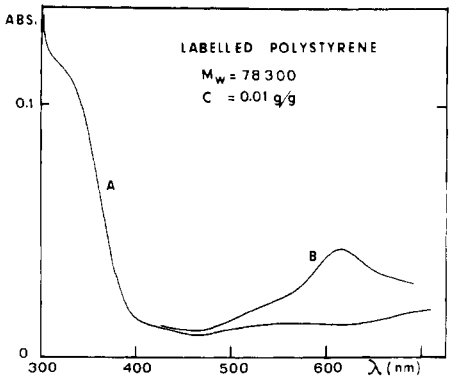

Figure 1. Absorbance vs. wavelength of labeled polystyrene chains in benzene solution for both nonphotoexcited (curve A) and photoexcited (curve B) forms.

1. Sample Preparation. We have used anionically prepared polystyrene samples which have been synthesized by Professor Rempp in Strasbourg. Their characteristics are listed in Table I. For each molecular weight, the living anionic polymer was divided into two parts. The first one was conventionally deactivated with methanol while the other one was deactivated with a solution of photochromic spiropyran molecules[13] (the 1′-(4-iodobutyl)-3′,3′-dimethylindolino-6-nitrobenzospiropyran was synthesized by Professor Gautron in Grenoble) to give polystyrene chains bearing one spiropyran molecule at each extremity. A typical absorption spectrum of labeled polystyrene chains in benzene solution is shown in Figure 1. The absorption maxima in the near-UV for the closed form and in the red for the open form are easily visible.

In order to keep the concentration of labeled chains small enough to avoid segregation, we prepared our samples by mixing a small amount of labeled chains with unlabeled chains of the same molecular weight. A dilute solution in benzene (spectroscopic grade) was then prepared, centrifuged at 20000g for 1 h to remove all dust particles, and brought to the desired final C by slow controlled evaporation of the solvent.

In all the present experiments, we assume that the interactions between the labeled macromolecules are negligible. Indeed, since the probe represents only a small fraction of the total chain (there are only two photochromic end groups for 10^3 or more monomers), the chemical potential of the photoexcited species is almost identical with that of the other chains. This has been confirmed experimentally by varying the concentration of labeled chains in the solution and by testing the invariability of the measured self-diffusion coefficient.

2. Experimental Setup. A block diagram of the experimental setup is shown in Figure 2. The periodic distribution of photoexcited molecules is created by illuminating the sample with an interference pattern. This pattern is produced by splitting the beam of a krypton laser (Coherent Radiation CR500K, λ_0 3507 Å) into two beams of equal intensity and recombining them in the sample. The interfringe spacing i is adjusted from 1 to 100 μm by varying the angle θ between the two beams. The Kr laser beam is mechanically chopped to give light pulses (from 1-ms to 1-s duration) with an adjustable repetition rate (from 20 ms to 30 min). The power of the exciting laser is generally kept below 10 mW. The reading laser is a 5-mW helium–neon laser (Spec-

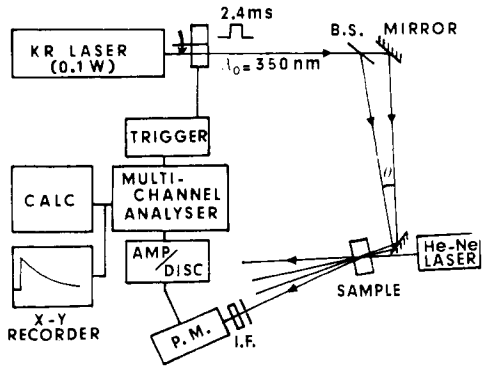

Figure 2. Block diagram of the experimental setup. The exciting laser beam (λ_0 350 nm) is split into two parts and recombined in the sample to form an interference pattern. The intensity diffracted by the photoinduced absorption grating is collected by the photomultiplier, averaged in the multichannel analyzer, and processed with the calculator.

tra-Physics Model 120, λ_1 6328 Å) further attenuated with a neutral density 3 in order to avoid any light-induced deexcitation of the spiropyran.[13] The polymer solution is contained in a spectroscopic cuvette with a 5-mm optical path. The absorbance of the photoexcited samples is always smaller than 0.3 at the reading wavelength. The corresponding extinction length d is large ($\simeq$1 cm), the ratio $K = 2\pi\lambda_1 d/ni^2$ (n is the refraction index of the cell) is much larger than 1, and we work in thick-grating conditions.[14] The incidence angle α of the reading laser has to be very carefully adjusted to the Bragg condition $2i\alpha = k\lambda_1$, within a few minutes of arc. The intensity diffracted in the first order is detected with a Radio Technique 56-TVP cooled photomultiplier, through a 0.5-mm pinhole. The phototube output pulses are amplified and fed into a Nicolet 1170 multichannel analyzer, triggered by the chopper. The relaxation of the diffracted intensity is thus recorded after each exciting light pulse, averaged over, and processed with a Hewlett-Packard 9825 calculator.

3. Data Processing. As usual in a light scattering experiment, the light diffracted by the periodic concentration of photoexcited molecules represents only a fraction of the total light received by the photodetector. The spontaneous, thermally excited, concentration fluctuations in the polymer solution and/or the stray light due to static imperfections of the cell walls give contributions which are by no means negligible. Since the photocathode is a quadratic detector, the coherence properties of the different scattered waves have to be taken into account, and the number of pulses, in the pulse counting mode, can be expressed by

$$n(t) = [Ae^{-t/\tau} + B]^2 + I^2 \quad (1)$$

$Ae^{-t/\tau}$ represents the amplitude of the diffracted field, and B and I are the amplitudes of the scattered fields which are respectively coherent and incoherent with the signal. One can notice that those two contributions are written as static ones, even if they contain a fraction of light scattered by concentration fluctuations in the solution. This assumption is valid since (i) their associated diffusion coefficient D_{coop} (which increases with increasing concentration) corresponds to a time constant much shorter than the one associated with the slow overall chain motion characterized by τ in eq 1 and (ii) they are not synchronized with the signal and their contribution can be averaged to a constant value.

Our data have been least-squares fitted to eq 1, with A, B, I, and τ as free adjustable parameters, for each decay curve. A typical intensity vs. time curve is shown in Figure 3, along with the deviation ϵ between experimental data points and calculated values. The adjustment has usually been performed on 200 points (which cover more than 4 time constants of the exponential), and we only retained experiments corresponding to a quality factor

$$Q = 1 - \sum_{i=1}^{N-1} \epsilon_i\epsilon_{i+1} / \sum_{i=1}^{N} \epsilon_i^2$$

better than 0.85 and to a χ^2 value smaller than 1.3.

It should be noted that these parameters only characterize the quality of the fit. The two preceding conditions ensure that our data are correctly described by eq 1, but they do not give any information on the accuracy to which the parameters A, B, I, and τ can be determined. This accuracy is essentially governed by the signal-to-noise ratio of the experiment, $R = (A^2 + 2AB)/B^2 + I^2$). For all our fits, τ is always derived with a relative uncertainty better than 3%. The other parameters are defined to a lesser precision, of the order of 10% in most instances, except when some of them (B or I) are much smaller than A. In that last case, however, the decrease in accuracy in the determination of B or I has no influence on τ, which is our primordial parameter.

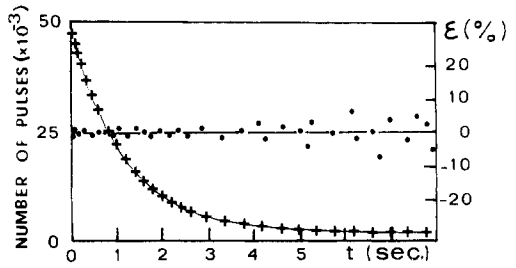

Figure 3. Typical plot of the diffracted intensity vs. time just after the flash excitation. The continuous line is the best fit to eq 1. The deviation ϵ between experimental and calculated values is also reported as an illustration of the quality of the fit (M_w = 754 000, C = 200 mg/g).

The following step is to deduce the self-diffusion coefficient D_{self} from the relaxation time τ of the diffracted intensity. The grating can disappear by two independent processes: (i) Brownian diffusion of the chains, which tends to equalize the induced spatial fluctuations of the photoexcited species toward the equilibrium uniform distribution; (ii) intramolecular relaxation by thermal deactivation of the photoexcited state. To distinguish between those two processes, we have measured the dependence of the relaxation time τ vs. the wave vector $q = 2\pi/i$ of the interference pattern. For a purely diffusive process, we expect $\tau^{-1} = D_{self}q^2$, while for a simple deexcitation of the dye, τ is independent of q: $\tau = \tau_d$. For any intermediate situation, we have a superposition of the two processes, and

$$\tau^{-1} = D_{self}q^2 + \tau_d^{-1} \quad (2)$$

Typical examples of the wave vector dependence of the relaxation time τ are shown in Figure 4 for purely diffusive processes (Figure 4A) or in a situation where both contributions are important (Figure 4B). The continuous line in Figure 4B is a least-squares fit to eq 2 from which we can extract both D_{self} and τ_d. The fitted value τ_d = 35 s is in good agreement with a direct photometric measurement of the time constant of the decrease of the absorption of the photoexcited sample at the reading wavelength, λ_1: τ_d = 30 ± 5 s.

II. Results

The concentration dependence of the self-diffusion coefficient D_{self} of polystyrene–benzene solutions is shown in Figure 5 for four different molecular weights. In all cases, a rapid decrease of D_{self} is observed when the concentration is increased above a limiting concentration C^*. For concentrations smaller than C^*, our results are in quantitative agreement with the translational diffusion coefficient obtained from ordinary Rayleigh light scattering.[4] Above C^*, we observe a linear decrease of D_{self}, in logarithmic scales, corresponding to a power law $D_{self} \sim C^{-\alpha}$, with α = 1.7 ± 0.1.

This behavior is in complete contrast with the ordinary Rayleigh light scattering (ORS) result. Since ORS is sensitive to the fluctuations in monomer concentration, it measures the cooperative diffusion coefficient D_{coop}, which increases with increasing concentration.[4] FRS is sensitive to the fluctuations in photoexcited chains, i.e., to the translational diffusion of the center of mass of the chains. Entangled polymer solutions provide thus a good illustration of the originality of FRS as compared to ORS and show how these two techniques can probe very different physical properties.

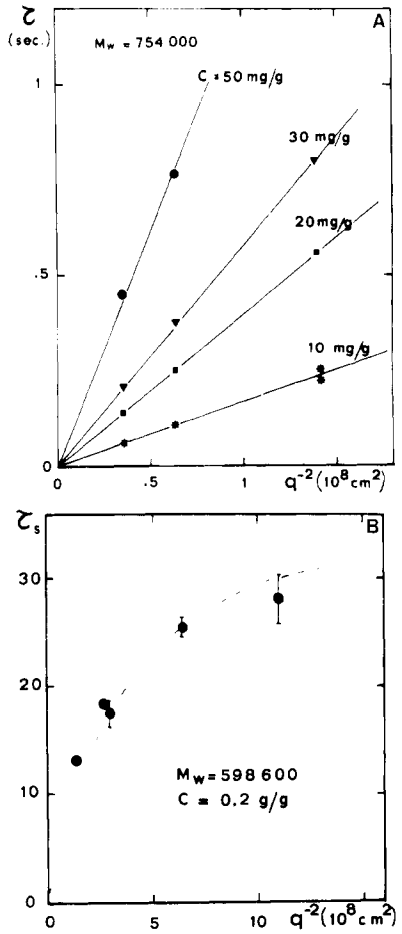

Figure 4. Wave vector dependence of the relaxation time τ for different samples. (A) Plots are shown for different concentrations of polystyrene of molecular weight 754 000. The linear behavior is characteristic of a purely diffusive process. (B) The saturation at large interfringe spacing corresponds to a relaxation of the grating by deexcitation of the spiropyran molecule. The dashed line is the best fit to eq 2 and yields τ_d = 35 s.

In Figure 6, we have reported the molecular weight dependence of the self-diffusion coefficient D_{self} for two different concentrations above C^*. A linear dependence is well observed, in logarithmic scales, over more than 2 decades. The corresponding β exponent in $D_{self} \propto \bar{M}^{-\beta}$ is 2.05 ± 0.1, where $\bar{M}$ is the mean value $\bar{M} = (M_w M_n)^{1/2}$. This rather unusual average comes from the fact that, for an absorption grating, the diffracted intensity I is proportional to the number of photoexcited molecules. Then, for a given distribution of polymerization index (with a number n_i of molecules of molecular weight M_i)

$$I(q,t) \propto \sum_i n_i e^{-D_{self\,i} q^2 t} / \sum_i n_i \qquad (3)$$

(in the case of a purely heterodyne detection)

The question is then to know which mean value of D_{self} is actually measured and how to relate it to a mean value of the molecular weight. Using a development in cumulants,[15] we can rewrite eq 3 as

$$I = e^{-\bar{D}_{self} q^2 t}\left[1 - q^2 t \frac{\sum_i n_i (D_{self\,i} - \bar{D}_{self})}{\sum_i n_i} + \frac{q^4 t^4}{2} \frac{\sum_i n_i (D_{self\,i} - \bar{D}_{self})^2}{\sum_i n_i} + \ldots\right]$$

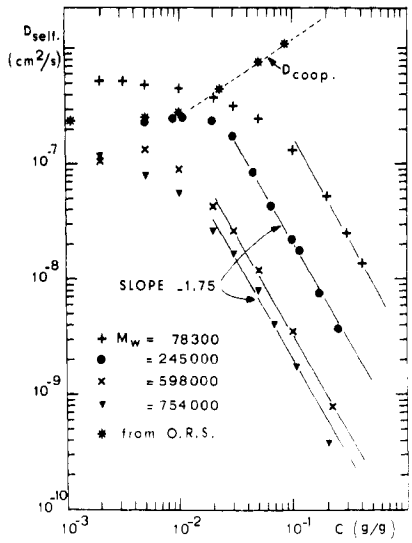

Figure 5. Concentration dependence of the self-diffusion coefficient of the chains for four different molecular weights in logarithmic scales. Above a limiting concentration C^* (depending on molecular weight) a linear decrease is observed, corresponding to $D_{self} \propto C^{-\alpha}$, with $\alpha = 1.7 \pm 0.1$. The asterisks show values of the translational diffusion coefficient for M_w = 270 000 and of the cooperative diffusion coefficient deduced from ref 4. All experiments have been performed at T = 22 °C.

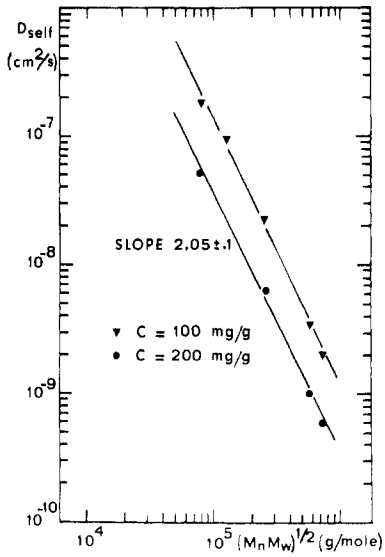

Figure 6. Molecular weight dependence of the self-diffusion coefficient D_{self} for concentrations C = 100 and 200 mg/g. The linear behavior, in logarithmic scales, corresponds to $D_{self} \propto \bar{M}^{-\beta}$, with $\beta = 2.05 \pm 0.1$.

where the mean value $\bar{D}_{self}$ is defined by the annulation of the second term of the development, i.e., by

$$\bar{D}_{self} = \sum_i n_i D_{self\,i} / \sum_i n_i \qquad (4)$$

We can notice that FRS is thus sensitive to a number average of the self-diffusion coefficient. This is quite different from the z average usually obtained in an ORS experiment

$$D_z = \sum_i n_i M_i^2 D_i / \sum_i n_i M_i^2$$

Assuming a power law dependence $D_{self\,i} \propto M_i^{-x}$, we obtain, with another development in cumulants

$$\bar{D}_{self} = (\text{constant}) \frac{1}{\bar{M}^x} \frac{\sum_i n_i [1 - (M_i^x - \bar{M}^x)/\bar{M}^x + \ldots]}{\sum_i n_i} \qquad (5)$$

where $\bar{M}^x = \sum_i n_i M_i^x / \sum_i n_i$ in order to cancel the first-order term in the development. As we deal with a number average in the self-diffusion coefficient, we are automatically led to a number average of the molecular weight to the x power. We see that, because of the polydispersity, the x exponent cannot be determined directly from $\bar{D}_{self}$ since it also enters in the definition of the mean value of M which we must use to correctly analyze our results. We can show, however, that the exponent $x = +2$ predicted by the reptation model is fully consistent with our data. Indeed, for $x = 2$, eq 5 predicts

$$\bar{D}_{self} \propto 1/\bar{M}^2 = \sum_i n_i / \sum_i n_i M_i^2 = (\sqrt{M_w M_n})^{-2}$$

in full agreement with the experimental results reported in Figure 6.

III. Discussion

1. Scaling Approach. A crude description of the motion of one chain in an entangled polymer solution can be made by analogy with the problem of one chain trapped in a network,[3] replacing the average distance between cross-links by the mean distance between entanglements, ξ. The test chain is then constrained to reptate[10] in a tube defined by all the topological constraints imposed by its neighbors. The average diameter of the tube is ξ, and its curvilinear length $L_t = (N/g)\xi$, where g is the number of monomers in one subunit of size ξ. $g = \phi\xi^3$ (ϕ is the number of monomers per unit volume, proportional to the concentration C, defined as the mass of monomers per unit volume). The mobility of the chain along the tube, μ_t, is smaller than the mobility μ_1 of one subunit by a factor N/g: $\mu_t = \mu_1/(N/g)$, with $\mu_1 \propto 1/\eta_s\xi$ (η_s is the solvent viscosity). The diffusion coefficient along the tube, D_t, can be related to μ_t by an Einstein relation:

$$D_t = kT\mu_t = \frac{kT}{\eta_s\xi}\frac{g}{N} \tag{6}$$

If we define the reptation time T_R as the time for the chain to renew its configuration, i.e., to choose a completely new tube, we have

$$D_t T_R \propto L_t^2 = (N/g)^2\xi^2 \tag{7}$$

and

$$T_R \propto \frac{\eta_s}{kT}\left(\frac{N}{g}\xi\right)^3 \sim N^3\phi^{1.5} \tag{8}$$

During the time T_R the reptating chain moves along the tube over the curvilinear distance L_t. However, in real space, its center-of-mass displacement is much smaller and equal to the radius of the chain $R(\phi) = (N/g)^{1/2}\xi$ (ideal chain of subunits of size ξ). Then

$$D_{self}T_R \propto R^2(\phi) = (N/g)\xi^2 \tag{9}$$

and

$$D_{self} \propto \frac{kT}{\eta_s\xi}\left(\frac{g}{N}\right)^2 \sim N^{-2}\phi^{-1.75} \tag{10}$$

If we choose as more practical variables the concentration $C = m\phi$ (m is the mass of the monomer) and the molecular weight $M = mN$, the predicted concentration and molecular weight dependences of D_{self} become

$$D_{self} \propto M^{-2}C^{-1.75} \tag{11}$$

and are very close to our experimental results presented in Figures 5 and 6. However, this agreement raises several questions since the above model oversimplifies the description of the motions of the chain, especially by assuming that all entanglements are fixed.

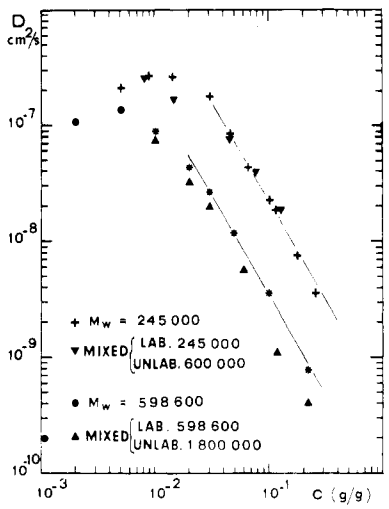

Figure 7. Comparison of the self-diffusion coefficient of labeled chains mixed with unlabeled chains of the same molecular weight or mixed with unlabeled chains of larger molecular weight, demonstrating the weakness of the tube renewal process in semidilute polymer solutions.

2. Influence of the Finite Lifetime of the Entanglements. In a real semidilute solution the entanglements are not fixed. The question is then to know if the motions of the surrounding chains can give another efficient process to renew the tube configuration. In a melt, this problem has been discussed independently by Klein[16] and Daoud and de Gennes.[17] Both concluded that the tube renewal is a very weak process. The basic process to change the tube configuration is to relax a topological constraint by changing the relative position of one of the surrounding chains with respect to the test chain. This can only be achieved when, by reptation, one extremity of a surrounding chain moves away from the test chain. Only a few such events appear during one reptation time of the test chain, with the result that the tube stays essentially fixed. To test that point, we have undertaken self-diffusion measurements in mixed systems, with labeled chains much shorter than the surrounding chains. One can expect that, for a large enough ratio of the molecular weights of unlabeled and labeled chains, the motions of the surrounding chains become completely frozen during the reptation time of the test chain ($T_R \propto M^3$ in the preceding scaling description). Results show that, within experimental error, when one labeled chain is mixed with unlabeled chains of the same molecular weight or up to 3 times larger (corresponding to a reptation time 1 order of magnitude larger) the chains have the same self-diffusion coefficient. These results are summarized in Figure 7 for two different molecular weights of labeled chains, M_w = 592 000 and M_w = 250 000, mixed with unlabeled chains of respectively M_w = 1 800 000 and M_w = 600 000. To the best of our knowledge, this gives the first experimental evidence of the weakness of the tube renewal process in a semidilute polymer solution (similar results have been reported recently in melt polyethylene[29]).

3. Comparison with Other Dynamical Measurements. Direct self-diffusion measurements in polymer systems are not very numerous. We can first notice that in the dilute concentration range, our results are in quantitative agreement with the translational diffusion coefficient obtained from ORS experiments[4] as shown for one molecular weight in Figure 5. In entangled solutions, D_{self} measurements have been performed very recently by Callaghan and Pinder,[18] using a pulsed field gradient nu-

clear magnetic resonance technique. Their data on the concentration dependence of D_{self} for one rather small (M_w = 110000) molecular weight of polystyrene seem compatible with the scaling description, though only few points on their curve correspond to the semidilute concentration range. The order of magnitude of their self-diffusion coefficients is the same as ours. On the other hand, their molecular weight dependence of D_{self} disagrees with the M^{-2} prediction in their experimental range, $10^5 \leq M_w \leq 2 \times 10^6$. It seems, however, that this result has to be taken with some caution. Their experiment is sensitive to both cooperative and individual chain motions, and the different contributions are not easy to separate, especially in the case of large molecular weights.

Bueche[19] and Kumagai et al.[20] have measured the self-diffusion coefficient in polystyrene melts, using radioactive tracers. Their results, for comparable molecular weights, are about 3 orders of magnitude smaller than what could be expected by a linear extrapolation toward $c = 1$ of our data of Figure 5. This discrepancy raises a serious question, and we have no definite answer at this stage. It could be simply remarked that (i) a linear extrapolation from the semidilute regime to the melt is certainly questionable. A departure from linearity at high concentration is detectable in Figure 5 for the largest molecular weight. Moreover, we know that eq 10 breaks down when the concentration increases. Daoud and de Gennes have shown that in the melt,[17] eq 10 must be corrected: the solvent viscosity has to be replaced by a monomer–monomer friction coefficient, and the size of the tube is now defined by the critical distance between entanglements $l_c = P_c^{1/2}a$ (P_c is the average number of statistical units between two entanglements, and a is the size of the statistical unit). In a simple scaling description, for $C \to 1$, ξ goes to a, with $a \ll l_c$. (ii) A critical examination of the work by Kumagai and coworkers shows that they typically follow the diffusion over distances of the order of 0.1–0.3 μm. This length scale is too small to completely exclude the possibility of diffusion processes dominated by the surface imperfections of their polymer films. The scarcity of details reported in Bueche's work prevents a meaningful discussion of his experimental results. D_{self} has been measured by Klein and Briscoe[21] in polyethylene melts and by Tanner[22] in poly(dimethylsiloxane) melts in situations where surface problems are unimportant (long diffusion length or spin-echo NMR). Their results fall in the range 10^{-9}–10^{-10} cm^2/s, much higher than the 10^{-13} cm^2/s reported by Kumagai and Bueche for comparable molecular weights. Further experiments in polystyrene melts are clearly needed to resolve these discrepancies.

If we now focus our attention on the molecular weight dependence of D_{self}, Tanner gives a power law $D_{self} \sim M^{-\alpha}$, with $\alpha = 1.7$, without correcting for polydispersity. On the other hand, Klein and Briscoe, working with highly polydisperse samples ($M_w/M_n \sim 2$) but correcting for it, have been able to find a power law $D_{self} \sim M^{-2}$, characteristic of a reptation process.

Thus self-diffusion measurements both in the melt[21] and in the semidilute concentration range (present work and concentration dependence of ref 18) seem to support the reptation plus scaling concepts. This approach, however, also predicts the molecular weight and concentration dependences of several other dynamical quantities, such as the terminal relaxation time τ_t or the zero-shear viscosity η_0, for which a very large amount of data is available.[23-26] τ_t deduced from viscoelastic measurements is the longest relaxation time of the semidilute solution and can be identified with T_R, while $\eta_0 = G_0T_R$, with an elastic modulus $G_0 \sim 1/\xi^3$. The scaling prediction for those two quantities is then

$$\tau_t \sim T_R \sim M^3C^{1.5}$$

$$\eta_0 \sim G_0T_R \sim M^3C^{3.75}$$

Experimentally, the commonly well-accepted result corresponds to an exponent 3.4 ± 0.1 for the molecular weight dependence, and the discrepancy is still larger (exponent 4.5 ± 0.5 for the viscosity) for the concentration dependence. We have no definite explanation for that discrepancy between the self-diffusion and the viscosity or relaxation measurements. Polydispersity may be a crucial factor. Recent experiments by Adam and Delsanti[24] have shown that polydispersity can affect significantly the exponent of the molecular weight dependence, even if narrow fractions are used. Their corrected result, $\eta_0 \sim M_w^{3\pm0.5}$, is indeed compatible with the reptation model. Moreover, it is clear that viscoelastic measurements are never performed strictly at mechanical equilibrium. The chains are always submitted to a finite shear. This may account for a part of the discrepancy, since the weakest entanglement points may be broken by the imposed strain, and the extrapolation to zero shear rate may be tricky. This is certainly one important advantage of the forced Rayleigh scattering technique, in which we do not mechanically disturb the sample.

Another result deduced from our self-diffusion measurements deserves mention. If we admit that a concentration dependence of $C^{-1.75}$ and a molecular weight dependence of M^{-2} are characteristic of a reptation process, i.e., of an entangled system, then we are led to the conclusion that all the molecular weights studied present an entangled behavior above a certain critical concentration. This critical concentration, even if not accurately defined for all molecular weights, is quite close to the values obtained in other measurements, either static[2] or dynamic[5] and is of the same order of magnitude as an evaluation from $C^* = M/R_g^3$. If we now focus our attention on the lowest studied molecular weight, M_w = 78000, we can see in Figure 6 that we do observe an entangled behavior for concentrations larger than 10^{-1} g/g. This is at variance with the plateau modulus and the viscosity measurements since they display a lowest critical molecular weight for entangled behavior M_c, with $M_cC \simeq$ 18000 or 30000, respecitvely, for polystyrene.[27] An explanation of that discrepancy can again come from the fact that self-diffusion measurements are performed at mechanical equilibrium. Anyway, it provides an illustration of the fact that the distinction recently proposed by Graessley[28] between semidilute not entangled and semidilute entangled regimes, based on viscosity measurements, may be delicate. The size of the semidilute nonentangled regime may be strongly dependent on the experimental method. A point of view more consistent with the scaling approach would be to imagine that regime as a crossover region between the dilute and the semidilute entangled regimes, the size of the crossover region depending on the property under consideration.

Conclusion

Using a forced Rayleigh light scattering technique, we have measured the self-diffusion coefficient of polystyrene chains in benzene in the semidilute concentration range. Our results for both concentration and molecular weight dependences are in very good agreement with the reptation model and the scaling predictions. We have shown, working on mixed systems where the labeled chains are shorter than their neighbors, that the reptation is the essential process in the motion of the chains. We are now

extending the experiment to Θ-solvent conditions, where it should give information on the relative importance of intrachain and interchain entanglements on chain motions.

One of the main limitations of the experiment comes from the fact that, for chemical reasons, we are not able to synthesize labeled molecules of very large molecular weight. We then have to work at rather large polymer concentrations. This could be questionable for the polystyrene–benzene system, as the proximity of the glass transition temperature could introduce additional contributions not taken into account in the scaling approach. Additional experiments on polyisobutylene, for which T_g is very low, could allow a test of that point.

Our experiments demonstrate the originality of the forced Rayleigh scattering technique. In the case of entangled polymer solutions, it gives information on physical properties completely different from those deduced from ordinary quasi-elastic Rayleigh light scattering. The latter technique is sensitive to monomer concentration fluctuations, i.e., to cooperative motions of the chains, while FRS is sensitive to individual chain motions. It is a quite interesting tool in the study of entangled polymer chains since it allows one (i) to measure dynamical properties at mechanical equilibrium and (ii) to specifically follow one of the components in mixed systems.

References and Notes

(1) Daoud, M., et al. *Macromolecules* **1975**, *8*, 804.
(2) de Gennes, P. G. "Scaling Concepts in Polymer Physics"; Cornell University Press: Ithaca, N.Y., 1979; Chapter III.
(3) de Gennes, P. G. *Macromolecules* **1976**, *9*, 594.
(4) Adam, M.; Delsanti, M. *Macromolecules* **1977**, *10*, 1229.
(5) Destor, G.; Rondelez, F. *J. Polym. Sci., Polym. Lett. Ed.* **1979**, *17*, 527.
(6) Munch, J. P., et al. *J. Phys. (Paris)* **1977**, *38*, 971.
(7) Pouyet, G., et al. *Macromolecules* **1980**, *13*, 176.
(8) Weill, G.; des Cloizeaux, J. *J. Phys. (Paris)* **1979**, *40*, 99.
(9) Vidakovic, P.; Allain, C.; Rondelez, F. *J. Phys. (Paris), Lett.* **1981**, *42*, 323.
(10) de Gennes, P. G. *J. Chem. Phys.* **1971**, *55*, 572. "Scaling Concepts in Polymer Physics"; Cornell University Press: Ithaca, N.Y., 1979; Chapter VIII.
(11) Hervet, H.; Léger, L.; Rondelez, F. *Phys. Rev. Lett.* **1979**, *42*, 1681.
(12) Hervet, H.; Urbach, W.; Rondelez, F. *J. Chem. Phys.* **1978**, *68*, 2725.
(13) *Tech. Chem. (N.Y.)* **1971**, *3*, Chapter II.
(14) "Handbook of Lasers"; CRC Press: Cleveland, Ohio, 1971; p 557.
(15) Koppel, D. E. *J. Chem. Phys.* **1972**, *57*, 4814.
(16) Klein, J. *Macromolecules* **1978**, *11*, 852.
(17) Daoud, M.; de Gennes, P. G. *J. Polym. Sci., Polym. Phys. Ed.* **1979**, *17*, 1971.
(18) Callaghan, P. T.; Pinder, D. N. *Macromolecules* **1980**, *13*, 1085.
(19) Bueche, F. *J. Chem. Phys.* **1968**, *48*, 1410.
(20) Kumagai, Y.; Watanabe, H.; Miyasaka, K.; Hata, T. *J. Chem. Eng. Jpn.* **1979**, *12*, 1.
(21) Klein, J.; Briscoe, B. J. *Proc. R. Soc. London, Ser. A* **1979**, *365*, 53.
(22) Tanner, J. E. *Macromolecules* **1971**, *4*, 748.
(23) Graessley, W. W. *Adv. Polym. Sci.* **1974**, *16*.
(24) Adam, M.; Delsanti, M. *J. Phys. (Paris), Lett.* **1979**, *40*, L-523.
(25) Onogi, S., et al. *J. Polym. Sci., Part C* **1966**, *15*, 381.
(26) Berry, G. C.; Nakayasu, H.; Fox, T. G. *J. Polym. Sci., Polym. Phys. Ed.* **1979**, *17*, 1825.
(27) Graessley, W. W. *Adv. Polym. Sci.* **1974**, *16*, 55.
(28) Graessley, W. W. *Polymer* **1980**, *21*, 258.
(29) Klein, J. *Macromolecules* **1981**, *14*, 460.

Laser Photochemistry of Polymers Having 1,2-*trans*-Dicarbazolylcyclobutane Groups in Solution

Hiroshi Masuhara,* Hiroshi Shioyama, and Noboru Mataga

Department of Chemistry, Faculty of Engineering Science, Osaka University, Toyonaka, Osaka 560, Japan

Takashi Inoue, Noboru Kitamura, Toshio Tanabe, and Shigeo Tazuke

Research Laboratory of Resources Utilization, Tokyo Institute of Technology, Midori-ku, Yokohama 227, Japan.

Received March 11, 1981

ABSTRACT: Transient absorption spectra of polyurethanes, a polyacrylate, and a polymethacrylate having 1,2-*trans*-dicarbazolylcyclobutane groups were measured by a microcomputer-controlled N_2 gas laser photolysis system. The triplet–triplet absorption intensity of these polymers is weak compared to that of the monomer reference compound. Examining various possibilities, it is concluded that the intrapolymer S_1–S_1 annihilation is a main factor leading to this polymer effect. The excited polymers quenched by dimethyl terephthalate dissociate into ion radicals whose yields are related to the polymer structure. This ionic photodissociation of the polyurethane results in formation of a transient polyelectrolyte in organic solvents.

Introduction

Recently, primary photoprocesses of molecularly associated systems in solution have been studied in detail, revealing that their behavior is sometimes different from that of dilute homogeneous solutions. These results are worth studying since most practical systems with technical and biological importance involve the photoprocesses of molecular aggregate, membrane, microemulsion, micelle, and polymer systems. It is well-known that the photoprocesses in photosynthesis, vision, and biological clocks are coupled to their protein structural change. The photoinduced charge separation in solar cells, photoconductors, and photoimaging materials is the essential primary process for their operation.

In relation to the mechanisms of the above phenomena, we have investigated by laser photolysis the primary photoprocesses of polymers with pendant aromatic groups in solution.[1-5] Interesting dynamic behavior characteristic of the polymers has been observed, summarized as follows:[2,4,5] (1) Intense laser excitation produces several fluorescent chromophores in one polymer chain and their mutual interaction leads to efficient intrapolymer S_1–S_1 annihilation. (2) The addition of an electron acceptor converts more than one fluorescent chromophore into an

0024-9297/81/2214-1738$01.25/0